INFECTION AND IMMUNITY, Mar. 2008, p. 952–958 Vol. 76, No. 3
0019-9567/08/$08.00+0 doi:10.1128/IAI.00927-07

MyD88 Signaling Contributes to Early Pulmonary Responses to *Aspergillus fumigatus*▽

Camille Bretz,[1] Geoff Gersuk,[1] Sue Knoblaugh,[1] Neelkamal Chaudhary,[3] Julie Randolph-Habecker,[1] Robert C. Hackman,[1,2] Janet Staab,[1,3] and Kieren A. Marr[1,2,3]*

Fred Hutchinson Cancer Research Center, Seattle, Washington[1]; University of Washington Medical Center[2]; and Oregon Health and Science University, Portland, Oregon[3]

Received 6 July 2007/Returned for modification 19 July 2007/Accepted 11 November 2007

Toll-like receptors and the β-glucan receptor, dectin-1, mediate macrophage inflammatory responses to *Aspergillus fumigatus* through MyD88-dependent and -independent signaling mechanisms; however, pulmonary inflammatory responses in MyD88-deficient mice challenged with *A. fumigatus* are poorly defined. The role of MyD88 signaling in early pulmonary inflammation and fungal clearance was evaluated in C57BL/6J wild-type (WT) and MyD88-deficient (MyD88$^{-/-}$) mice. Early (<48 h) after infection, MyD88$^{-/-}$ mice had higher fungal burdens than those of WT mice, although fungal burdens rapidly declined (>72 h) in both. MyD88$^{-/-}$ mice had less consolidated inflammation, with fewer NK cells, in lung tissue early (24 h) after infection than did WT mice. At the latter time point, MyD88$^{-/-}$ mouse lungs were characterized by a large amount of necrotic cellular debris and fibrin, while WT lungs had organized inflammation. Although there were equivalent numbers of macrophages in WT and MyD88$^{-/-}$ mouse lung tissues, MyD88$^{-/-}$ cells demonstrated delayed uptake of green fluorescent protein-expressing *A. fumigatus* (GFP-Af293); histologically, MyD88$^{-/-}$ mouse lungs had more hyphal invasion of terminal airways and vessels, the appearance of bronchiolar epithelial cell necrosis, and necrotizing vasculitis. MyD88$^{-/-}$ lung homogenates contained comparatively decreased amounts of interleukin-1β (IL-1β), IL-6, KC, and gamma interferon and paradoxically increased amounts of tumor necrosis factor alpha and macrophage inflammatory protein 1α. These data indicate that the MyD88-dependent pathway mediates acute pulmonary fungal clearance, inflammation, and tissue injury very early after infection. Resolution of abnormalities within a 3-day window demonstrates the importance of redundant signaling pathways in mediating pulmonary inflammatory responses to fungi.

Molds are an important cause of opportunistic pulmonary infections in immunocompromised people, with recent studies finding that invasive pulmonary mold infections account for a bulk of infection-related morbidity after therapy for hematological malignancies and hematopoietic stem cell transplants (10). *Aspergillus fumigatus* is an especially important mold, given its frequent involvement in the majority of established lung infections and its contribution to inflammatory syndromes, including allergic bronchopulmonary aspergillosis and allergic asthma (10).

Recent efforts have focused on describing the cellular mechanism(s) by which hosts avoid pulmonary infection caused by the frequently inhaled fungus while modulating associated inflammation. A compelling body of evidence indicates that hosts (human and murine) rely upon Toll-like receptors (TLRs) and C-type lectins, such as dectin-1, to sense the presence of and respond to *Aspergillus* ligands (3, 4, 21). Multiple recent studies demonstrated that dectin-1, in cooperation with TLR2, mediates macrophage responses to hypha-exposed β-1,3-glucan (3, 4, 21). Other studies have implicated TLR4 in macrophage responses to *A. fumigatus*, although specific microbial ligands have not yet been identified (7, 14, 16). Results of in vitro studies suggest that these responses are mediated at least in part by MyD88-dependent signaling mechanisms (7, 23), although the in vivo phenotype associated with MyD88 deficiency is difficult to appreciate. Hence, studies that have evaluated the in vivo pulmonary response to *A. fumigatus* in MyD88-deficient animals have incorporated additional immunosuppression in order to measure comparative phenotypes after infection. Bellochio and colleagues reported that MyD88 deficiency in the presence of pharmacological immunosuppression led to lower survival rates and increased fungal burdens compared to those of wild-type controls (1). More recently, Dubourdeau and colleagues produced relatively contradictory evidence showing that MyD88 deficiency is not associated with either increased risk of death or differences in fungal burden (2).

Results of prior studies have utilized crude measures of the host response (e.g., survival) and have focused on pulmonary events that have occurred late (>3 days) after organism challenge (1, 2). However, multiple infection models have shown a time dependency of host pulmonary responses to inhaled pathogens, with sequential early events largely shaping the course of infection and inflammation. For example, TLR signaling through MyD88 appears to be critical for early inflammatory responses to bacterial pathogens such as *Pseudomonas aeruginosa*, yet MyD88-independent mechanisms ultimately allow for clearance of bacteria and inflammation (17, 18, 20). We hypothesized that redundant pathways exist to modulate infection and inflammation caused by *A. fumigatus*; as such, prior studies that evaluated responses in the setting of additional immunosuppression and/or measured effects late after infection could have underestimated the phenotype associated with

* Corresponding author. Mailing address: Oregon Health and Science University, Division of Infectious Diseases, 3181 SW Sam Jackson Park Rd., Mail Code NRC-03, Portland, OR 97239. Phone: (503) 418-1685. Fax: (503) 494-4264. E-mail: marrki@ohsu.edu.

▽ Published ahead of print on 26 November 2007.

MyD88 deficiency. To test this hypothesis, we challenged mice lacking MyD88 (MyD88$^{-/-}$) with green fluorescent protein (GFP)-expressing *A. fumigatus* to measure early events after pulmonary infection. The results suggest that MyD88-dependent signaling facilitates fungal clearance and coordination of inflammation and lung injury early after infection.

MATERIALS AND METHODS

Animals. MyD88-deficient mice on a C57BL/6J background were originally provided by S. Akira (Osaka University, Osaka, Japan). The mice were backcrossed eight times to specific-pathogen-free C57BL/6 wild-type (WT) mice and then bred to generation F6. Male mice (18 to 25 g) were used at 8 to 11 weeks of age. Animal care and studies were performed with the approval of the institutional animal care and use committee.

GFP-expressing *Aspergillus fumigatus*. The well-characterized clinical isolate *A. fumigatus* strain Af293 was used. In order to facilitate in vivo studies, we constructed an *Aspergillus fumigatus* Af293 strain (GFP-Af293) that constitutively expresses GFP. Briefly, plasmid GFP containing a synthetic version of the *GFP* gene (S65T) (8) and two separate glyceraldehyde 3-phosphate promoters (driving constitutive expression of the *Escherichia coli* hygromycin B resistance gene) was linearized at a unique ClaI (Invitrogen) site and transformed into Af293 by electroporation (24). Transformants were passaged several times in medium containing hygromycin B to select for stable integration of the plasmid. Conidia from hygromycin-resistant clones were restreaked on potato dextrose agar (PDA; Becton Dickinson) for 2 to 3 days at 30°C, harvested by being flushed with phosphate-buffered saline (PBS) containing 0.05% Tween 80, and examined for GFP expression by light and epifluorescence microscopy using a Nikon Eclipse TE300 microscope equipped with standard fluorescein isothiocyanate (FITC) filters and a Cool-Snap digital camera (Meridian Instrument).

Experimental infection. Mice were infected by the inhalation route, using an aerosol chamber created by a 1-liter Pyrex flask with eight tubular glass side arms fitted at a 30° angle and spaced equidistantly around the flask (6). Prior to infection, inhalation flasks were sterilized, seeded with a suspension of *A. fumigatus* conidia (1×10^8 conidia/ml) on PDA, and incubated at 30°C for 6 days to produce a fungal lawn. Conidia were aerosolized by pumping air into the flask, using a 60-ml syringe attached to Tygon tubing. To minimize variability in pulmonary inocula, WT and MyD88$^{-/-}$ mice were infected in the same flasks and then randomly assigned to different time groups. Inoculum controls were evaluated 1 hour after exposure. Pilot experiments were performed to determine that a 90-second exposure time delivered a reproducible number of conidia per mouse within and between experiments, with a mean of 3.4×10^6 CFU recovered per lung.

Measures of fungal burden. Quantification of viable *A. fumigatus* cells within the lungs of infected mice was performed by CFU counts. At 1, 6, 24, 48, and 72 h postinfection, mice were euthanized, and lungs were removed aseptically, weighed, and homogenized in 2 ml of sterile PBS with a tissue homogenizer (Dremel, Racine, WI). Serial dilutions of the tissue homogenates were plated onto PDA plates without antibiotics. CFU were calculated per lung homogenate and weight of tissue. Only *A. fumigatus* colonies were observed on the plates. The remaining homogenate was tested by quantitative PCR and galactomannan assays to confirm quantitative assessments, using previously described methods (19).

Measurement of inflammatory mediators in lung homogenates. Mouse tumor necrosis factor alpha (TNF-α) and interleukin-12 p70 (IL-12p70) protein levels were quantified using commercially available enzyme-linked immunosorbent assay (ELISA) kits according to the manufacturer's instructions (eBioscience). A Bio-Plex suspension array system (Bio-Rad Laboratories, Hercules, CA) was used to measure a broader panel of cytokines and chemokines in lung homogenates (IL-1β, IL-4, IL-6, IL-10, gamma interferon [IFN-γ], macrophage inflammatory protein 1α [MIP-1α], MIP-1β, MIP-2, macrophage chemoattractant protein 1 [MCP-1], and KC).

Histopathology and cell populations. Animals were anesthetized and euthanized, and necropsy was performed immediately to minimize the effects of tissue destruction. Organs were inspected to detect any gross anomalies. Lungs were removed under aseptic conditions, weighed, and homogenized. A part of each specimen was fixed in 10% formalin and embedded in paraffin. Blocks were cut into 4-μm sections and stained with hematoxylin-eosin and Gomori's methenamine silver to examine fungal morphology.

Expression of GFP was measured using a Zeiss LSM 510 confocal microscope with LSM software to produce two-color (red and green) images (for green imaging, a 488-nm laser was used, with a 500- to 530-nm detection wavelength; for red imaging, a 543-nm laser was used, with a 565- to 615-nm detection wavelength) to distinguish GFP fluorescence from autofluorescence. Image-J software (http://rsb.info.nih.gov/ij/) was used to arrange all images. Stacks were employed to overlay fluorescent and phase-contrast light images.

Separate experiments were performed to compare cellular populations in lung homogenates 24 and 48 h after infection. Mice were sacrificed (three mice per group per time point), and lung tissues were sliced and incubated with RPMI 1640 containing type III collagenase (150 U/ml; Worthington Biochemical Corporation, NJ) and type I DNase (50 U/ml; Sigma), with 5% fetal calf serum, 100 U/ml penicillin, 100 μg/ml streptomycin, and 10 mM HEPES. After 1.5 h of incubation at 37°C (in 5% CO_2), a single-cell suspension was obtained by pipetting. Erythrocytes were lysed using 1× red blood cell lysis buffer (BD Pharmingen, San Diego, CA). Cells were washed twice with wash buffer (PBS with 0.1% NaN_3 and 1% fetal calf serum), and viable cells were counted using trypan blue. Cells were suspended in the wash buffer at a concentration of 4×10^7 cells/ml. Immunostaining for cell surface molecules was performed for 30 min at 4°C, using antibodies against CD3 (CD3/17A2-FITC), CD4 (CD4-L3T4/GK1.5-phycoerythrin [PE]), CD8b (CD8b-Ly-3/H35/17.2-PE), CD49b (CD49b/PanNK/DX5-PE), Ly6-G/Ly6-C (Ly-6G/Ly-6C–PE), CD11C (CD11c/HL3-FITC), and F4/80 (F4/80-PE). All antibodies except for F4/80-PE (eBiosciences, San Diego, CA) were purchased from BD Pharmingen (San Diego, CA). The concentrations of antibodies were optimized in preliminary experiments, and isotype controls were included. After being stained, cells were washed twice in wash buffer and fixed in 1% paraformaldehyde (Fisher Scientific, Pittsburgh, PA). Lung cell suspensions were then analyzed by flow cytometry using a FACSCalibur flow cytometer (Becton Dickinson Immunocytometry Systems, San Jose, CA) and analyzed using CellQuest software (Becton Dickinson).

Statistical analysis. Based on CFU calculations in pilot experiments, it was calculated that a sample size of 12 mice in each group was needed to have a 90% power to detect a difference of 1.4 standard deviations between groups, with a 0.05 two-sided significance level. All data are expressed as means ± standard errors of the means (SEM). Differences in measured variables between MyD88$^{-/-}$ mice and the control group were measured using Student's *t* test, when appropriate. Differences were considered significant at *P* values of <0.05.

RESULTS

MyD88 deficiency impairs pulmonary clearance of *A. fumigatus* early after infection, with associated dysregulation of early pulmonary inflammatory response. The pulmonary fungal burden was measured by quantification of CFU 1, 6, 24, 48, and 72 h after infection (Fig. 1a). No differences were noted between WT and MyD88$^{-/-}$ mice at early time points (Fig. 1a and data not shown). The burden was higher in MyD88$^{-/-}$ animals 72 h after infection. Histopathologic examination of lung tissue demonstrated a difference by 72 h after challenge, with the MyD88$^{-/-}$ mice having prominent hyphae, with invasion of bronchial walls. In contrast, rare hyphae were seen in the WT mouse airways or lung tissue by 72 h after challenge (Fig. 1b and c). Differences in pulmonary fungal burden were verified using a galactomannan enzyme immunoassay and quantitative PCR (data not shown).

The lung parenchyma was examined by histopathology of mice sequentially after exposure to *A. fumigatus* conidia. At 1 hour postinoculation, the WT and MyD88$^{-/-}$ lung sections were histologically normal, with the exception of the presence of a few to many intraluminal conidia in scattered airways (data not shown). Six hours after exposure, lung sections remained histologically normal, although conidia were apparent within terminal airways (data not shown). By 24 h, the WT lung sections contained early scattered areas of inflammation, characterized by an accumulation of neutrophils within small vessels, capillaries, and scattered airways and the multifocal appearance of neutrophils within vessel lumens (Fig. 2a, inset). In more severely affected areas, neutrophils accumulated within alveolar spaces, with mild necrosis apparent. In the WT lung

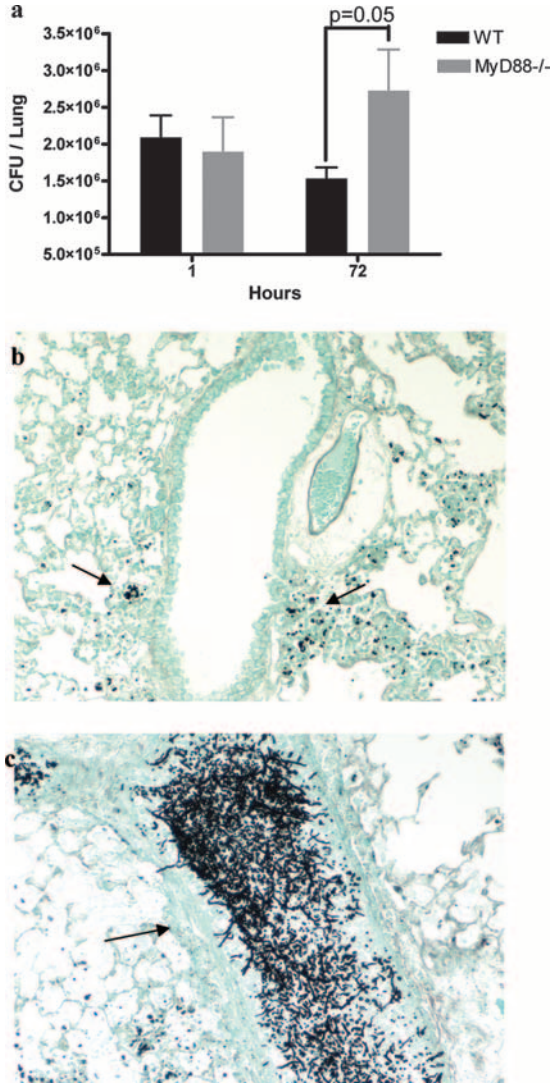

FIG. 1. *Aspergillus fumigatus* fungal burdens in lungs of WT and MyD88$^{-/-}$ mice differ early after infection. Animals were exposed to *A. fumigatus* by inhalation, as described in the text. (a) Fungal burdens were quantified by measurement of CFU. Data are means (± SEM) for three independent experiments containing four mice per condition (total $n = 12$). Data are presented relative to those for total lungs; the weights of lungs over time for WT and MyD88$^{-/-}$ mice did not differ over time (data not shown). Representative histopathological sections with Gomori's methenamine silver staining of lungs (magnification, ×20) from mice infected 72 h earlier demonstrated essentially clear airways in WT mice, with conidia visible in the lung parenchyma (b, arrows), and hyphal elements visible in small and large airways of MyD88$^{-/-}$ mice, where hyphae were disrupting and expanding bronchiolar walls (c, arrows). *P* values shown are two-sided and were calculated from Student's *t* test.

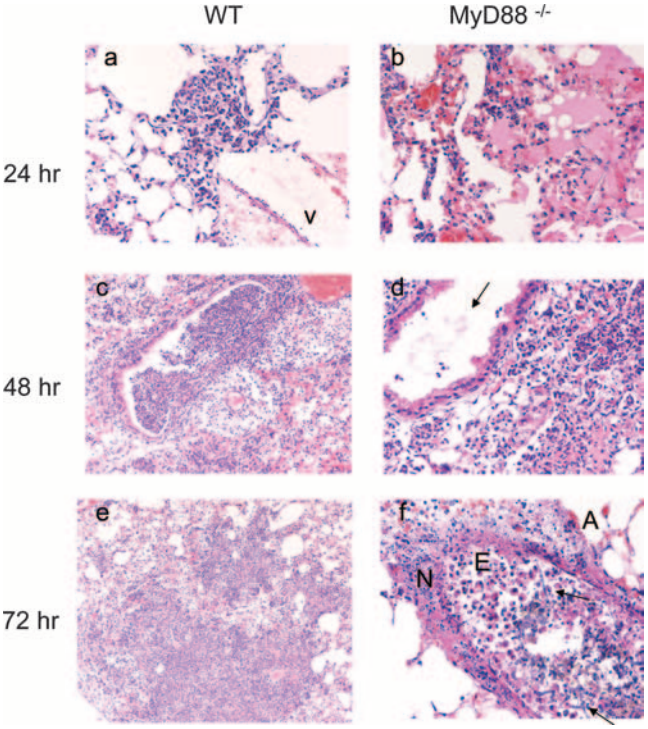

FIG. 2. Representative sections of lungs from WT (left) and MyD88$^{-/-}$ (right) mice are shown at the indicated times after infection with *A. fumigatus* conidia. Sections were stained with hematoxylin and eosin and visualized at the indicated magnifications. Mild necrosis and neutrophils were seen within alveolar spaces 24 h after infection in the WT (a) (×40) mice. Margination of neutrophils was apparent within vessels (inset; magnification, ×40). Conidia were apparent within macrophages (not shown). In the MyD88$^{-/-}$ mice, inflammation and neutrophils were present in a more scattered distribution (b) (×40), with larger amounts of edema. In the WT mice, segmental necrosis of airways with perivascular edema was present by 28 h (c) (×20). At 48 h, the MyD88$^{-/-}$ mice (d) (×60) had areas of segmental necrosis, edema, and fibrin. Scattered areas of consolidated inflammation were present in the WT sections at 72 h (e) (×10). The MyD88$^{-/-}$ sections (f) (×20) contained areas of segmental necrosis of bronchioles with intraluminal fungal hyphae (arrows), cellular debris and necrosis (N), and sloughed bronchiolar epithelial cells (E). Images were obtained from one mouse per time point. A, alveoli.

sections, conidia were visualized within macrophages (Fig. 2a). In MyD88$^{-/-}$ lung sections, inflammatory foci were apparent, but in a more scattered distribution in the lung. Within these foci, inflammation was more severe, with the focal presence of necrosis, edema, and free fungal organisms noted within alveolar spaces and airways (Fig. 2b). There did not appear to be phagocytized fungal organisms within macrophages.

By 48 h, inflammation in the WT lung sections had become more severe and consolidated. The affected areas existed within close proximity to minimally affected or normal areas (Fig. 2c). In this sense, the lesional areas were consolidated and localized. The affected areas were characterized by degenerate and nondegenerate neutrophils within and surrounding airways and vessels, with edema, and by few free and phagocytized conidia; no hyphae were present. There was perivascular and peribronchiolar edema with ectatic lymphatics and multifocal segmental necrosis. In the MyD88$^{-/-}$ sections, inflammation was similar in character but less severe, with less localization and consolidation of the inflammatory response. Severely affected areas contained segmental necrosis of airways, degenerate and nondegenerate neutrophils, edema, and fibrin within airways and alveolar spaces (Fig. 2d). At this point, there were some alveolar macrophages that contained intracytoplasmic conidia.

Differences were most notable 72 h after infection. In the WT lung sections, there were scattered localized and consoli-

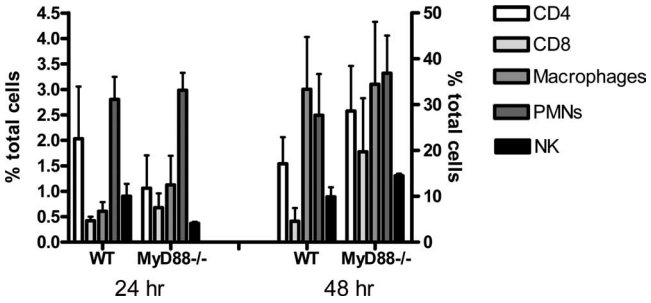

FIG. 3. Cell populations in lung homogenates at the indicated times after infection with *A. fumigatus* conidia. Percentages of total cells were graphed relative to the left *y* axis for CD4 and CD8 T lymphocytes (both also $CD3^+$) and macrophages ($F4/80^+$), and PMNs ($Ly\text{-}6G/Ly\text{-}6c^+$) and NK cells ($CD49b^+$) were graphed relative to the right *y* axis. Data are shown for two experiments, using three mice each (means ± SEM).

dated areas of inflammation, similar to those described at 48 h. These areas were characterized by mild necrosis, degenerate and nondegenerate neutrophils, and few macrophages containing intracytoplasmic conidia; still, no hyphae were apparent (Fig. 2e). In the $MyD88^{-/-}$ lung sections, the inflammation was scattered and less pronounced; however, there was striking

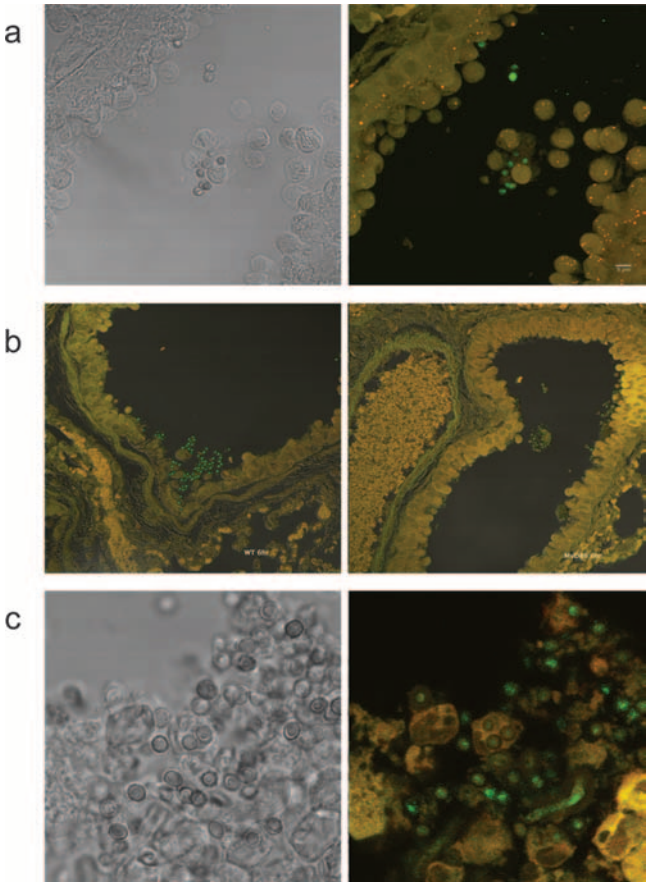

FIG. 4. Representative sections of lung tissue from WT and $MyD88^{-/-}$ mice after exposure to GFP-Af293. Montage images are shown for WT (a) and $MyD88^{-/-}$ (b) mice exposed to GFP-Af293 1 h prior to imaging.

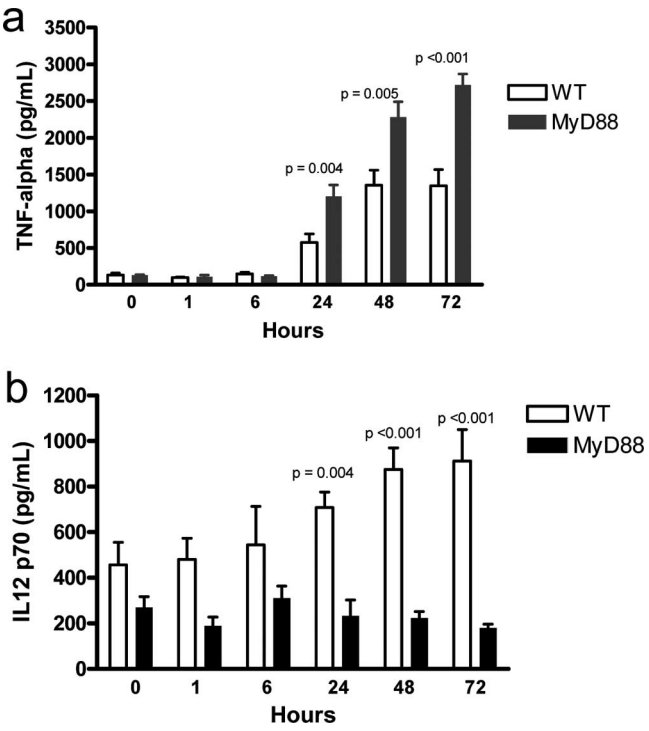

FIG. 5. TNF-α (a) and IL-12p70 (b) were quantified from lung homogenates at all early time points, using ELISA. Data shown are means for 8 to 12 animals assessed in three different experiments, with SEM. *P* values shown are two-sided and were calculated by comparison between $MyD88^{-/-}$ and WT means, using Student's *t* test. Data points without *P* values indicate values of >0.05.

vascular involvement. This was characterized by necrotizing vasculitis with segmental disruption and expansion of vessel walls with fibrin, abundant cellular debris, and invading hyphae. There was also multifocal necrosis of bronchioles with abundant intraluminal cellular debris, hyphae, and sloughed bronchiolar epithelial cells (Fig. 2f).

The cellular compositions of lung homogenates were assessed by flow cytometry (Fig. 3). There were no differences in the numbers of $CD4^+$ and $CD8^+$ T cells, macrophages, and polymorphonuclear leukocytes (PMNs) recovered from $MyD88^{-/-}$ mice and WT mice both early (24 h) and later (48 h) after infection. There was a trend toward fewer NK cells in the lungs of $MyD88^{-/-}$ mice than in those of WT mice ($P = 0.07$) at the earlier time point, although the numbers normalized later.

Histological examination suggested differences in macrophage uptake of conidia in WT and $MyD88^{-/-}$ lungs. To examine early intracellular events in more detail, mice were infected with GFP-Af293, and lung tissues were visualized by fluorescence (Fig. 4). GFP-expressing *A. fumigatus* was evident in airways of both WT and $MyD88^{-/-}$ mice as early as 1 h after exposure (Fig. 4a). Conidia appeared to be predominantly intracellular in alveoli of WT (Fig. 4a) and $MyD88^{-/-}$ (not shown) mice. By 6 h after challenge, most conidia were intracellular in the airways; organisms that remained extracellular in both WT and $MyD88^{-/-}$ mice were predominantly adherent to bronchial columnar epithelial cells (Fig. 4b). Clear differences in fungal morphology and location were apparent by 72 h

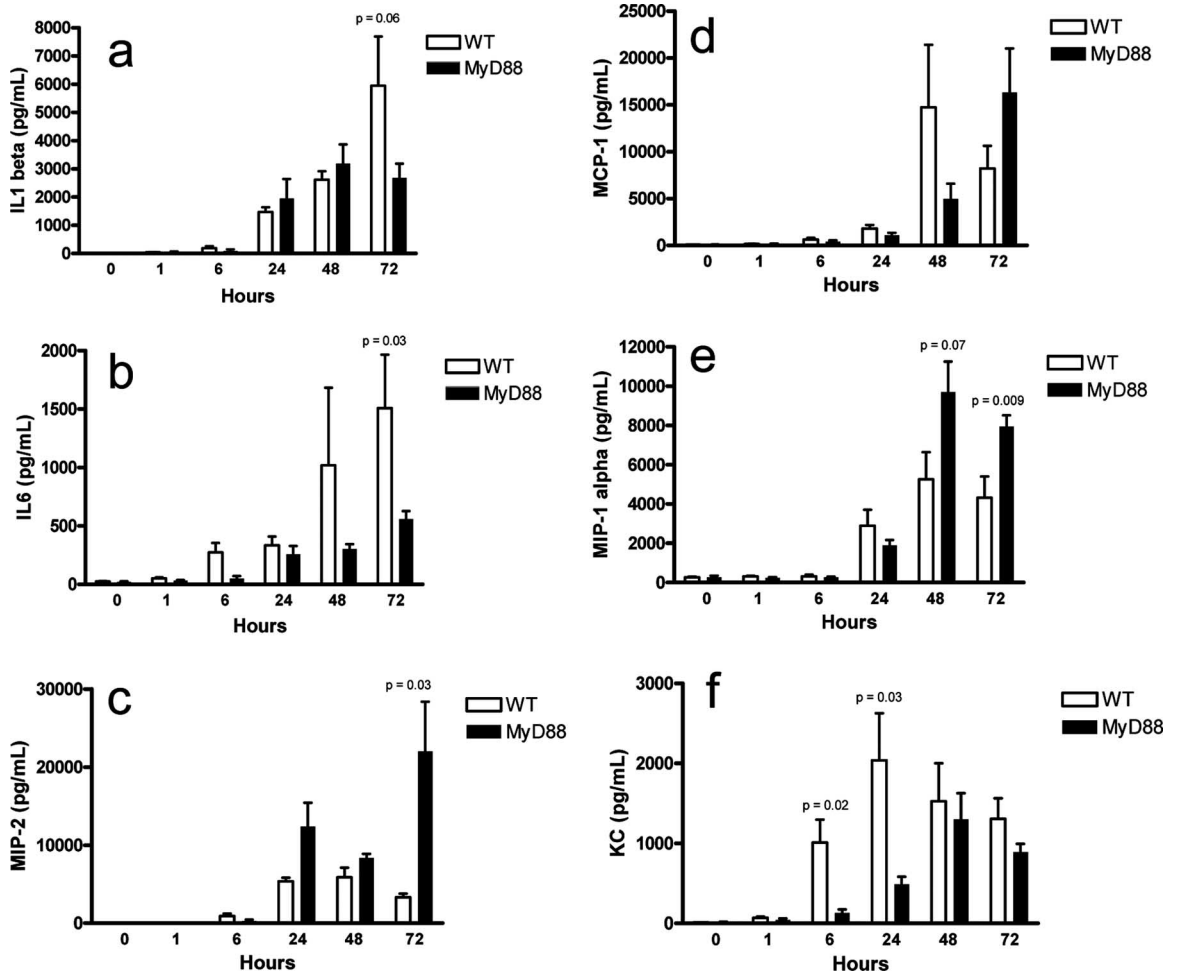

FIG. 6. BioPlex assays were performed to measure IL-1β (a), IL-6 (b), MIP-2 (c), MCP-1 (d), MIP-1α (e), and KC (f) from WT and MyD88$^{-/-}$ lung homogenates sampled at the indicated time points after infection with *A. fumigatus*. Data shown are means for 8 to 15 mice assessed in three different experiments, with SEM. *P* values shown are two-sided and were calculated by comparison between MyD88$^{-/-}$ and WT means, using Student's *t* test. Data points without *P* values indicate values of >0.05.

after challenge. In the WT mice, no GFP-Af293 could be visualized; in contrast, sections of MyD88$^{-/-}$ mouse lungs contained abundant swelling and germinating conidia, both intracellularly in the airways (Fig. 4c) and extracellularly, within the parenchyma of the lungs (not shown).

TNF-α and IL-12p70 in lung homogenates were quantified using ELISA (Fig. 5); early after Af293 challenge, WT lungs contained relatively greater quantities of IL-12p70. In contrast, MyD88$^{-/-}$ lungs accumulated relatively greater amounts of TNF-α. A broader profiling of the cytokine and chemokine composition in lung homogenates was performed by BioPlex assays, specifically focusing on mediators that have been implicated in responses in invasive and/or allergic aspergillosis models. As shown in Fig. 6, lung homogenates recovered from WT mice contained relative greater amounts of IL-6, IL-1β, and KC, especially early after infection. Lung homogenates from MyD88$^{-/-}$ mice contained relatively larger quantities of MIP-2 and MIP-1α. Small amounts (<10 pg/ml) of IFN-γ were recovered in the lung homogenates of either the WT or MyD88$^{-/-}$ mice at early time points; by 72 h, IFN-γ was increasing in WT mice (mean, 99.3 pg/ml), but it increased less so in the MyD88$^{-/-}$ lung homogenates (mean, 14 pg/ml; $P = 0.002$). Very little (<50 pg/ml) IL-4 or IL-10 was recovered from lung homogenates of either group at any time point. The relatively higher level of TNF-α in the MyD88$^{-/-}$ lung homogenates was confirmed by BioPlex assay (data not shown).

Histological evidence of lung damage in MyD88-deficient mice. As shown in Fig. 2, fibrin began accumulating in the airways of MyD88$^{-/-}$ mice 48 h after challenge. Later, there was segmental disruption and expansion of bronchiolar walls, with necrotic debris. In contrast, WT mice had focal areas of consolidation with no apparent destruction of the airway epithelium.

DISCUSSION

In prior studies, investigators reported that MyD88$^{-/-}$ mice challenged with *A. fumigatus* demonstrate no innate differences in infection susceptibility, as measured by survival or fungal burden assessed late (>3 days) after organism challenge (1, 2). In those studies, the MyD88$^{-/-}$ mice demonstrated differences in phenotype only after added pharmacologic im-

munosuppression. We hypothesized that the lack of appreciable defects was due to insensitivity in the model outcomes measured (e.g., survival) and because redundant pathways compensate in clearing organisms and modulating pulmonary inflammation over time. The studies shown here suggest that MyD88-dependent pathways mediate pulmonary fungal clearance, inflammation, and associated lung injury very early after infection. The results expand upon our knowledge of in vivo processing of inhaled fungi and provide in vivo correlates to the role(s) of MyD88-dependent pathways demonstrated in vitro (1, 2).

In one previous study, Bellocchio and colleagues assessed the functional significance of MyD88-mediated signaling in an *Aspergillus* conidium nasal challenge model; MyD88$^{-/-}$ mice immunosuppressed with cyclophosphamide had increased pulmonary fungal burdens and rates of death compared to WT mice (1). In a more recent study, Dubourdeau and colleagues reported that no differences in survival were measured in MyD88$^{-/-}$ and WT mice after *A. fumigatus* challenge, even in the setting of immunosuppression with cortisone acetate, with no major differences in histopathology 4 days after infection or conidial killing of macrophages harvested from bronchoalveolar lavage fluid (2). These studies outline the conflicting nature of our current knowledge concerning the role of MyD88 signaling in mediating killing of and inflammatory responses to *A. fumigatus*; other in vitro studies have similarly generated different conclusions from experiments that measured cytokine secretion after organism challenge (7, 9). The data presented in this study expand upon our current knowledge of the role of MyD88 signaling in pulmonary immune responses to *A. fumigatus*; while clear differences in fungal burden and inflammation were present very early after infection, many of the measured abnormalities were relatively normalized within 3 days after pulmonary challenge. This finding is likely explained by the redundant nature of signaling pathways in mediating inflammatory responses. Indeed, several MyD88-independent pathways have been shown to mediate macrophage responses to *A. fumigatus* ligands, including those mediated by dectin-1-syk (3, 4, 21) and the mitogen-activated protein kinase extracellular signal-regulated kinase (2). An appreciation of the role of each pathway in in vivo studies appears to be dependent on subtle differences in experimental design, such as the timing of assessments and degree of additional pharmacological immunosuppression, and on sensitive measures of in vivo cellular interactions.

Using a GFP-expressing organism, the in vivo studies herein showed that intracellular processing of conidia was different in macrophages from WT and MyD88$^{-/-}$ lungs; specifically, MyD88$^{-/-}$ macrophages demonstrated delayed phagocytosis and decreased clearance of *A. fumigatus* conidia. These data are consistent with the results of studies that have implicated a role for MyD88-dependent pathways in conidial phagocytosis and killing, using cells harvested from WT and MyD88-deficient mice (3, 4, 21). Our data indicate that these pathways are likely to be most important very early after pulmonary infection; however, it is difficult to determine how much of the measured defect is associated with differences in secondary inflammatory responses and cellular recruitment, as opposed to macrophage function per se. Nonetheless, the response of the MyD88$^{-/-}$ mouse was insufficient to contain organisms in the conidial state, as occurred in the WT mouse; instead, hyphal vascular and airway invasion and tissue necrosis were apparent within 3 days after infection.

The histopathology performed in this study was purely descriptive, with few mice examined per time point. Nonetheless, we observed marked differences in the type of inflammation, with a more disorganized pattern of consolidation evident in the MyD88$^{-/-}$ mice. While quantification of cellular populations did not show large differences in subtypes present in WT and MyD88$^{-/-}$ infected lungs, there were small numbers of NK cells found at early time points; this finding is consistent with the observed differences in the mediators MIP-2 and MCP-1 (13, 15). These results also support those of another study that demonstrated a role for NK cells in the early pulmonary defense against aspergillosis (15), although the exact role of NK cells in the antifungal response has yet to be defined.

In this model, MyD88 signaling appeared to be particularly important for later stages of inflammatory consolidation and prevention of lung injury. This is not unlike what was recently demonstrated for *Pseudomonas* pulmonary infection models, in which MyD88-dependent and -independent signaling was involved sequentially during early and late pulmonary responses. Specifically, MyD88-dependent signaling is important in mediating late (24 to 48 h) PMN recruitment and the production of MIP-2, TNF-α, and IL-1α (17, 18). Also, similar to the case after *A. fumigatus* infection, MyD88$^{-/-}$ mice challenged with *P. aeruginosa* develop late cellular necrosis and the appearance of fibrin-based coagulum in the airways (20). Further studies would be necessary to characterize the nature (and progression) of lung injury.

The findings of increased tissue damage and the appearance of extracellular matrix components in *P. aeruginosa*- and *A. fumigatus*-challenged MyD88$^{-/-}$ mice are worthy of further discussion. These observations are consistent with dysregulated repair of tissue injury. Since *A. fumigatus* hyphae can directly invade the bronchial epithelium, injury is likely both inflammatory and infectious in origin. Of note is the recent observation that MyD88-dependent signaling plays a role in regulating noninfectious lung injury, sustained by bleomycin disruption of epithelial cell surface hyaluronan (5). A TLR-MyD88-dependent signaling mechanism(s) mediates lung epithelial cell repair. Hence, decreased fungal killing in MyD88-deficient mice may not be the only defect leading to the observed lung injury. While hyphal disruption of the bronchial epithelium likely serves to augment the overall damage observed in the MyD88$^{-/-}$ lung, it is also possible that deficiencies in MyD88-dependent signaling, with associated impaired epithelial cell repair, lead to increased susceptibility to fungal airway damage.

An important finding of this study is the observation that inflammatory mediators were present in different quantities in the WT and MyD88$^{-/-}$ lung homogenates. Of particular interest is the paradoxical increase in TNF-α, MIP-2, and MIP-1α observed in MyD88$^{-/-}$ lung homogenates, as all of these mediators have previously been shown to play a role in the pulmonary defense against *A. fumigatus* (11–13, 15). The results of recent studies have shown that dectin-1 mediates the production of these cytokines, through both MyD88-dependent and -independent pathways (3, 4, 21). However, macro-

phages generate responses primarily through recognition of β-glucan present on the hyphal form of the organism. Hence, this paradoxical increase may well be a dectin-1-dependent, MyD88-independent secondary response that results from an increased hyphal burden in the lung. It is important that in this study, cytokines and cell populations were measured in lung homogenates, not in bronchoalveolar lavage fluid, and the compartmentalized responses may be different. Our findings also suggest that the elaboration of certain cytokines and chemokines in response to *A. fumigatus* is likely to be more or less dependent on β-glucan recognition, verifying the roles of other receptors in mediating pulmonary inflammatory responses to *A. fumigatus*.

MyD88 not only mediates signaling through TLRs that have been implicated in *Aspergillus* defenses (TLR2 and TLR4) but also mediates signaling via the IL-1 receptor; defining precisely which pathway is involved in the observed differences requires further study. Determining the important defect will be complicated further by the recent observation that MyD88 mediates stabilization of IFN-γ-induced transcripts encoding TNF-α and IFN-γ-inducible protein 10 (22).

In conclusion, this study documents that MyD88 plays a role in mediating inflammatory responses to *A. fumigatus* early after pulmonary infection. The fungal burden is increased, largely associated with decreased and delayed conidial clearance in the MyD88-deficient animal. In addition, MyD88-dependent pathways mediate the coordination of inflammation and tissue repair early after pulmonary infection with *A. fumigatus*. Since many disease states caused by *Aspergillus* species result largely from dysregulated pulmonary inflammation, mechanisms of signaling may actually play a role in disease pathogenesis.

ACKNOWLEDGMENTS

We thank Joe Fedynyshyn and Maria Mariana (Bio-Rad) for performance of BioPlex assays and Leon Razai and Kendra Garrison for technical assistance.

This study was supported by NIH grant R01 AI051468 to K.A.M.

REFERENCES

1. **Bellocchio, S., C. Montagnoli, S. Bozza, R. Gaziano, G. Rossi, S. S. Mambula, A. Vecchi, A. Mantovani, S. M. Levitz, and L. Romani.** 2004. The contribution of the Toll-like/IL-1 receptor superfamily to innate and adaptive immunity to fungal pathogens in vivo. J. Immunol. **172:**3059–3069.
2. **Dubourdeau, M., R. Athman, V. Balloy, M. Huerre, M. Chignard, D. J. Philpott, J. P. Latge, and O. Ibrahim-Granet.** 2006. Aspergillus fumigatus induces innate immune responses in alveolar macrophages through the MAPK pathway independently of TLR2 and TLR4. J. Immunol. **177:**3994–4001.
3. **Gersuk, G. M., D. M. Underhill, L. Zhu, and K. A. Marr.** 2006. Dectin-1 and TLRs permit macrophages to distinguish between different Aspergillus fumigatus cellular states. J. Immunol. **176:**3717–3724.
4. **Hohl, T. M., H. L. Van Epps, A. Rivera, L. A. Morgan, P. L. Chen, M. Feldmesser, and E. G. Pamer.** 2005. Aspergillus fumigatus triggers inflammatory responses by stage-specific beta-glucan display. PLoS Pathog. **1:**e30.
5. **Jiang, D., J. Liang, J. Fan, S. Yu, S. Chen, Y. Luo, G. D. Prestwich, M. M. Mascarenhas, H. G. Garg, D. A. Quinn, R. J. Homer, D. R. Goldstein, R. Bucala, P. J. Lee, R. Medzhitov, and P. W. Noble.** 2005. Regulation of lung injury and repair by Toll-like receptors and hyaluronan. Nat. Med. **11:**1173–1179.
6. **Loebenberg, D., A. Cacciapuoti, R. Parmegiani, E. L. Moss, Jr., F. Menzel, Jr., B. Antonacci, C. Norris, T. Yarosh-Tomaine, R. S. Hare, and G. H. Miller.** 1992. In vitro and in vivo activities of SCH 42427, the active enantiomer of the antifungal agent SCH 39304. Antimicrob. Agents Chemother. **36:**498–501.
7. **Mambula, S. S., K. Sau, P. Henneke, D. T. Golenbock, and S. M. Levitz.** 2002. Toll-like receptor (TLR) signaling in response to Aspergillus fumigatus. J. Biol. Chem. **277:**39320–39326.
8. **Maor, R., M. Puyesky, B. Horowitz, and A. Sharon.** 1998. Use of the green fluorescent protein (GFP) for studying development and fungal-plant interaction in Cochliobolus heterostrophus. Mycol. Res. **102:**491–496.
9. **Marr, K. A., S. A. Balajee, T. R. Hawn, A. Ozinsky, U. Pham, S. Akira, A. Aderem, and W. C. Liles.** 2003. Differential role of MyD88 in macrophage-mediated responses to opportunistic fungal pathogens. Infect. Immun. **71:**5280–5286.
10. **Marr, K. A., T. Patterson, and D. Denning.** 2002. Aspergillosis. Pathogenesis, clinical manifestations, and therapy. Infect. Dis. Clin. N. Am. **16:**875–894.
11. **Mehrad, B., T. A. Moore, and T. J. Standiford.** 2000. Macrophage inflammatory protein-1 alpha is a critical mediator of host defense against invasive pulmonary aspergillosis in neutropenic hosts. J. Immunol. **165:**962–968.
12. **Mehrad, B., R. Strieter, and T. Standiford.** 1999. Role of TNF-α in pulmonary host defense in murine invasive aspergillosis. J. Immunol. **162:**1633–1640.
13. **Mehrad, B., R. M. Strieter, T. A. Moore, W. C. Tsai, S. A. Lira, and T. J. Standiford.** 1999. CXC chemokine receptor-2 ligands are necessary components of neutrophil-mediated host defense in invasive pulmonary aspergillosis. J. Immunol. **163:**6086–6094.
14. **Meier, A., C. J. Kirschning, T. Nikolaus, H. Wagner, J. Heesemann, and F. Ebel.** 2003. Toll-like receptor (TLR) 2 and TLR4 are essential for Aspergillus-induced activation of murine macrophages. Cell. Microbiol. **5:**561–570.
15. **Morrison, B. E., S. J. Park, J. M. Mooney, and B. Mehrad.** 2003. Chemokine-mediated recruitment of NK cells is a critical host defense mechanism in invasive aspergillosis. J. Clin. Investig. **112:**1862–1870.
16. **Netea, M. G., A. Warris, J. W. Van der Meer, M. J. Fenton, T. J. Verver-Janssen, L. E. Jacobs, T. Andresen, P. E. Verweij, and B. J. Kullberg.** 2003. Aspergillus fumigatus evades immune recognition during germination through loss of Toll-like receptor-4-mediated signal transduction. J. Infect. Dis. **188:**320–326.
17. **Power, M. R., J. S. Marshall, M. Yamamoto, S. Akira, and T. J. Lin.** 2006. The myeloid differentiation factor 88 is dispensable for the development of a delayed host response to Pseudomonas aeruginosa lung infection in mice. Clin. Exp. Immunol. **146:**323–329.
18. **Power, M. R., Y. Peng, E. Maydanski, J. S. Marshall, and T. J. Lin.** 2004. The development of early host response to Pseudomonas aeruginosa lung infection is critically dependent on myeloid differentiation factor 88 in mice. J. Biol. Chem. **279:**49315–49322.
19. **Sheppard, D. C., K. A. Marr, D. N. Fredricks, L. Y. Chiang, T. Doedt, and S. G. Filler.** 2006. Comparison of three methodologies for the determination of pulmonary fungal burden in experimental murine aspergillosis. Clin. Microbiol. Infect. **12:**376–380.
20. **Skerrett, S. J., C. B. Wilson, H. D. Liggitt, and A. M. Hajjar.** 2007. Redundant Toll-like receptor signaling in the pulmonary host response to Pseudomonas aeruginosa. Am. J. Physiol. Lung Cell. Mol. Physiol. **292:**L312–L322.
21. **Steele, C., R. R. Rapaka, A. Metz, S. M. Pop, D. L. Williams, S. Gordon, J. K. Kolls, and G. D. Brown.** 2005. The beta-glucan receptor dectin-1 recognizes specific morphologies of Aspergillus fumigatus. PLoS Pathog. **1:**e42.
22. **Sun, D., and A. Ding.** 2006. MyD88-mediated stabilization of interferon-gamma-induced cytokine and chemokine mRNA. Nat. Immunol. **7:**375–381.
23. **Wang, J. E., A. Warris, E. A. Ellingsen, P. F. Jorgensen, T. H. Flo, T. Espevik, R. Solberg, P. E. Verweij, and A. O. Aasen.** 2001. Involvement of CD14 and Toll-like receptors in activation of human monocytes by *Aspergillus fumigatus* hyphae. Infect. Immun. **69:**2402–2406.
24. **Weidner, G., C. d'Enfert, A. Koch, P. C. Mol, and A. A. Brakhage.** 1998. Development of a homologous transformation system for the human pathogenic fungus Aspergillus fumigatus based on the pyrG gene encoding orotidine 5′-monophosphate decarboxylase. Curr. Genet. **33:**378–385.

Editor: A. Casadevall